Energy and Buildings 133 (2016) 79–87

Contents lists available at ScienceDirect

Energy and Buildings

journal homepage: www.elsevier.com/locate/enbuild

Event-driven optimization of complex HVAC systems

Junqi Wang [a], Gongsheng Huang [a,*], Yongjun Sun [b], Xiaoping Liu [c]

[a] Department of Architecture and Civil Engineering, City University of Hong Kong, Hong Kong
[b] Division of Building Science and Technology, City University of Hong Kong, Hong Kong
[c] School of Civil Engineering, Hefei University of Technology, Hefei, Anhui, China

ARTICLE INFO

Article history:
Received 11 March 2016
Received in revised form 11 August 2016
Accepted 20 September 2016
Available online 21 September 2016

Keywords:
Event-driven optimization
Real-time optimization
HVAC systems
Energy efficiency
Computational efficiency

ABSTRACT

Real-time optimization (RTO) has been developed to improve the cost and/or energy efficiency of complex heating, ventilation and air-conditioning (HVAC) systems. In current literature, almost all of the developed real-time optimization methods belong to the type of time-driven optimization, in which the action of optimization is triggered by "time". As optimization should be done when the system operating conditions experience a change that is large enough to cause current operational setting not optimal any more, optimization strategies should recognize 'significant' changes and perform optimization when necessary. Since the time-driven optimization is a periodic mechanism in nature while those 'significant' changes may not be periodic, the time-driven optimization cannot capture 'significant' changes and do the optimization promptly. Therefore, this paper proposes an event-driven optimization (EDO) for complex HVAC systems, the key idea of which is to use "event" rather than "time" to trigger the action of optimization. A systematic event-driven optimization method is illustrated, where its main tasks, including event definition and event identification, will be discussed. The proposed method will be compared with a conventional time-driven method using case studies, through which the main advantages of the proposed method will be identified.

1. Introduction

Heating, ventilation and air-conditioning (HVAC) systems contribute the significant part (20–50%) of building energy consumption [1]. It is worthwhile to consider real-time optimization (RTO) in HVAC systems since large energy savings could be obtained from a small improvement in operating efficiency [2]. Real-time optimization is a type of optimization that optimizes control settings or variables (or decision variables) to minimize or maximize a predefined cost function [3]. It has been used in HVAC systems since the 1980s [4]. In the 1990s, most studies focused on the real-time optimization of the local loops or subsystems of HVAC systems using classic linear/quadratic programming, or gradient-based iterative methods [5,6]. Recently, to address the complexity of large-scale HVAC systems, advanced optimization algorithms have been developed, such as evolutionary algorithms [7], branch and bound [8], simulated annealing [9], and so on. ASHRAE handbook surveyed the publications since 1980s [10]; and new developments till 2008 were reviewed by Wang and Ma [11].

In the real-time optimization of HVAC systems, the majority of the developed methods belong to the type of time-driven methods, in which the actions of optimization are triggered by "time" periodically whether using a fixed optimization frequency or a scheduled timetable, *i.e.* the optimization will be done at predefined time instants according to current available information. For example, Kusiak et al. [12] investigated the real-time optimization of air handling unit (AHU), in which the supply air pressure and temperature were optimized every hour. They showed that 7.66% of the total energy consumption can be reduced. Mossolly et al. [13] tested the hourly optimization of the fresh air flow rate and the supply air temperature in a VAV system and demonstrated that 30.4% of the energy consumption can be reduced over the summer season (4 months). Yoon et al. [14] developed a real-time optimization strategy for a double-skin façade system, in which the blind slat angel, airflow regime and opening ratio were optimized every 15 min to achieve the minimal energy consumption. In the work of Zaheeruddin and Zheng [15], 24-h operation was divided into three modes based on time: night set-back mode (5:00 P.M.–7:00 A.M.), start-up mode (7:00 A.M.–8:00 A.M.), and normal mode (8:00 A.M.–5:00 P.M.). The optimization actions were only performed when the operation mode was changed.

In a time-driven method, a suitable optimization frequency is important for the performance of optimization [16]. Basically, a

* Corresponding author.
E-mail address: gongsheng.huang@cityu.edu.hk (G. Huang).

http://dx.doi.org/10.1016/j.enbuild.2016.09.049
0378-7788/

higher frequency will lead to a better performance because the response to the variation of operating conditions is faster [17]. However, it is known that optimization should be done when system operating conditions experience a significant change that causes current operational settings not optimal any more [10]. Therefore, an optimization strategy should recognize 'significant' changes and performance the optimization accordingly only when necessary. As the time-driven optimization is a periodic mechanism in nature while those 'significant' changes may not be periodic (actually they are stochastic and difficult to predict), the time-driven optimization may not capture 'significant' changes and do the optimization promptly. Although one can choose an extremely high optimization frequency such that the random change can be captured with minor delay, a higher frequency will increase the computation burden, which will be critical when the system computational resource is limited, especially for a large-scale system where a number of decision variables are taken into account [18,19]. Besides, a higher frequency may waste the computational resource when operating conditions are stable and optimization is not necessary (but still be performed) [20,21]. Therefore, a new control optimization mechanism is needed, which should recognize 'significant' changes and perform the optimization only when necessary.

In this paper, an event-driven optimization (EDO) method is proposed. The key idea of the event-driven optimization is to use "event" rather than "time" to trigger the action of optimization. It should be noted that the event-driven method (also known as "event-based" or "event-triggered") is not a new concept. It originates from the study of discrete event systems [22]. A nice feature of the event-driven paradigm is that it is able to follow the stochastic behavior of system operation, and thus increasing the flexibility of control, communication and optimization [23]. Previous studies have already shown that event-driven mechanism can reduce the computation load effectively while simultaneously ensure the control or optimization performance. For example, without sacrificing the performance, 50% reduction of computation load was achieved in [24] and 70–80% of computation reduction was achieved in [25]. These studies have demonstrated the potential of event-driven control.

It is noticed that until now there is very few studies on this specific topic on the feasibility of applying event-driven optimization to HVAC systems. As the operation of HVAC systems usually confronts many stochastic and unpredicted 'state transmission', such as weather condition changes, load changes and occupancy changes, "time" may not be a good driver for the real-time optimization. Given the potential of event-driven optimization, this paper develops a framework of event-driven optimization for HVAC applications and evaluates its performance by comparing with the conventional time-driven optimization. Firstly, the event-driven optimization is illustrated in a systematic way, where its main tasks, including event definition and event identification, are discussed. Then, case studies are conducted to demonstrate the application potential of the event-driven optimization in HVAC systems. The performances of the event-driven and time-driven optimization are compared, based on which the main advantages of the proposed method will be discussed.

2. Event-driven optimization

2.1. Basic framework

The framework of the event-driven optimization is illustrated in Fig. 1. The event space is a collection of events that will be used to trigger the action of optimization, which should be defined before the implementation. The occurrence of an event is identified through analyzing real-time operational data or monitoring data. If an event is identified, control optimization will be executed to find optimal values of decision variables with respect to concerned objectives. Otherwise, no action will be taken. Note that optimization algorithms that are developed for time-driven method can also be used to optimize decision variables in this framework.

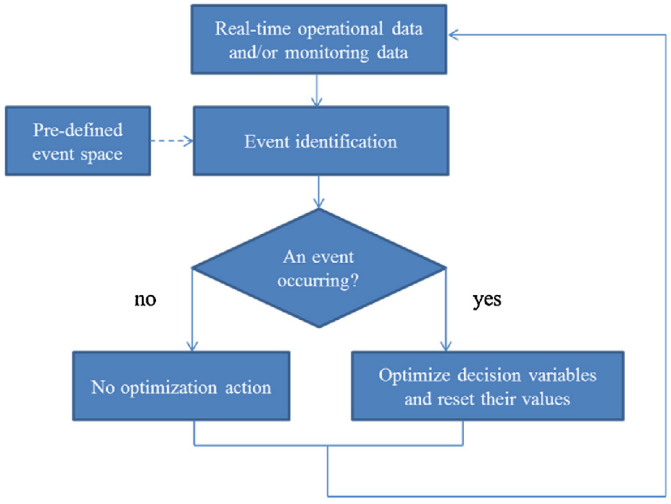

Fig. 1. The framework of event-driven optimization.

2.2. Event definition

To achieve the real-time optimization in an event-driven manner, defining events is vital since it decides when to take the action and will significantly affect the system performance. Basically, an "event" should be defined as something physically happening which can reflect the system state transition [22]. For example, a chiller being switched on can be considered as an 'event'; and the cooling load increased by 10% can be considered as an event as well. Hence, 'event' can be defined naturally from a digital state (e.g. the status on/off of chiller), or a continuous state (e.g. the cooling load):

$$e := \begin{cases} \eta\left(x_{t_0} \rightarrow x_{t_1}\right) > \sigma_e & \text{for continuous state transition} \\ \eta_{t_1} \neq \eta_{t_0} & \text{for digital state transition} \end{cases} \quad (1)$$

where η is the state corresponding to the event; x is a set of variables that can be used to reflect the event state; σ_e is a predefined threshold; t_1 indicates the current decision time; and t_0 indicates the last decision time.

In daily operation of a complex HVAC system, events may come from environment (such as weather changes and solar radiation changes), system itself (such as equipment on/off, equipment faults and operation mode changes) and occupants (such as occupancy changes and occupants' adjustment of thermal comfort related variables), which can be regarded as different sources of events. As not all of 'state transition' should be used as 'events' to trigger optimization, only those 'state transitions' which could cause a significant influence on concerned objectives (such as energy efficiency) will be defined as events. The collection of all the events forms an event space as below:

$$E_{space} := \left\{e_1, \cdots, e_N\right\} \quad (2)$$

Prior knowledge, computer simulation and/or operational data analysis (e.g., data mining) should be resorted to find the importance of 'state transition' with respect to concerned optimization objectives (such as energy use). It should be noted that for events with continuous states, thresholds are necessary for the definition. A suitable threshold may depend on the particular system that is

under consideration. Once again, computer simulation and operation data analysis are powerful tools to find the suitable threshold.

2.3. Event identification

After events have been defined, the event space is established and can be used to trigger the optimization. Meanwhile, in real applications, a mechanism of identifying the occurrence of an event should also be established. As an event is in nature a state transition whether in a digital form or continuous form, a simple identification mechanism is developed as

For continuous state:

$$e = \begin{cases} 0, \eta\left(x_{t_0} \to x_{t_1}\right) \le \sigma_e \\ 1, \eta\left(x_{t_0} \to x_{t_1}\right) > \sigma_e \end{cases} \quad (3)$$

For digital state:

$$e = \begin{cases} 0, \eta_{t_1} = \eta_{t_0} \\ 1, \eta_{t_1} \ne \eta_{t_0} \end{cases} \quad (4)$$

where '$e = 1$' indicates the occurrence of an event; while '$e = 0$' indicates no event was detected.

For example, when the part-load ratio (PLR) of a chiller plant has changed by 10% compared with the last optimization, it is defined as an event. x is defined as $x = \left(m_w, T_{chw,rtn}, T_{chw,sup}\right)$ since the cooling load Q is calculated by

$$Q = c_p m_w \left(T_{chw,rtn} - T_{chw,\sup}\right) \quad (5)$$

where c_p is the specific thermal capacity of chilled water; m_w is the mass flow rate of chilled water; $T_{chw,rtn}$ is the chilled water return (CHWR) temperature and $T_{chw,sup}$ is the chilled water supply (CHWS) temperature. Then the state transition η becomes

$$\eta\left(x_{t_0} \to x_{t_1}\right) = \left|\frac{Q_{t_1} - Q_{t_0}}{Q_{rated}}\right| \quad (6)$$

where Q_{rated} is the rated cooling capacity of the operating chillers. As the threshold σ_e is 10%, this event will be detected when $\eta$is larger than 10%.

In a digital state example, suppose '0′ indicates off, '1' indicates on and the initial state η_{t_0} is '0'. If a chiller being switched on or off is defined as an event, this event will be detected if η_{t_1} becomes '1'.

2.4. Real-time optimization algorithm

In the real-time optimization of HVAC systems, an objective function and decision variables should be firstly defined. The objective function will be maximized or minimized by finding optimal values of decision variables with respect to current operational condition. In practice, operational or other type of constraints should be taken into account [10]. In this study, an HVAC system of all-electric cooling without thermal storage (with primary and secondary chilled water loops) is considered, which is a commonly used commercial system. Please note that minimizing power requirement at each point in time is equivalent to minimizing energy costs [10], and thus the objective function becomes the minimization of the system power which is formulated in Eqs. (7) and (8):

$$P_{sys,tot} = P_{ch,tot} + P_{ct,tot} + P_{pump,tot} + P_{fan,tot} = P_{sys,tot}\left(T_{cw}, T_{chw,prm}, T_{chw,\sec}, T_{sa}, U\right) \quad (7)$$

$$\left(T^*_{cw}, T^*_{chw,prm}, T^*_{chw,\sec}, T^*_{sa}\right) = \underset{T_{cw}, T_{chw,prm}, T_{chw,\sec}, T_{sa}}{\arg\min} P_{sys,tot} \quad (8)$$

where P is the power and T is the temperature; subscripts *sys, tot, ct, pump* and *fan* represent system, total, cooling tower, pump, and fan; subscripts *cw, chw, prm, sec* and *sa* represent cooling water, chilled water, primary, secondary and supply air; the superscript '*' represents the corresponding optimal values of decision variables; and U is the vector of uncontrolled variables (e.g., ambient air temperature).

Here four decision variables are considered, including the set-points of cooling water supply (CWS) temperature, CHWS temperature from chiller(s), CHWS temperature from heat exchanger(s) and supply air (SA) temperature, because these four variables have been found very important for the energy performance of HVAC systems and their optimal values vary with the operation conditions by many studies [10,18,26]. The system total power requirement can be written as a function of these four decision variables based on the performance models of chiller, cooling tower, AHU, heat exchanger, pump and fans. Details of the performance models are shown in the reference [26]. The constraints are shown in Eqs. (7)–(12), where the Eqs. (7)–(10) indicates lower and upper bounds for four temperature set-points. Two additional constraints are adopted as shown in (11) and (12). Constraint (11) sets the maximal temperature difference cannot be larger than a threshold value (e.g., 0.5 °C) and is used to prevent the system instability caused by large set-point changes [26]. Constraint (12) is to ensure a minimal temperature difference between the primary and secondary sides of the chilled water loops.

$$T_{cw,low} \le T_{cw,e} \le T_{cw,up} \quad (7)$$

$$T_{chw,prm,low} \le T_{chw,prm,e} \le T_{chw,prm,up} \quad (8)$$

$$T_{chw,\sec,low} \le T_{chw,\sec,e} \le T_{chw,\sec,up} \quad (9)$$

$$T_{sa,low} \le T_{sa,e} \le T_{sa,up} \quad (10)$$

$$\left|T_{e(k+1)} - T_{ek}\right| \le \Delta T_{Thres} \quad (11)$$

$$T_{chw,prm,e} + \Delta T_{\min} \le T_{chw,\sec,e} \quad (12)$$

3. Case study

The proposed EDO was illustrated through a case study. In this section, the case HVAC system and the simulation platform were introduced. Load profiles and operational constraints were also presented.

3.1. Description of the case AC system

The AC system contains an air distribution system, a loop of cooling water, and two loops of chilled water. The system schematic is shown in Fig. 2. Heat exchangers are used to guarantee a proper water pressure in the primary and secondary water loops respectively. The cooling towers are used to dissipate the heat collected from indoor space; while the AHUs are used to cool down supply air and deliver the conditioned supply air to each zone. To guarantee a proper system operation, several fundamental controls are necessary and are briefly explained as follows [26].

3.1.1. Sequencing control of chillers

This is to stage on or off chillers based on a given load condition. Here, a total-cooling-load-based sequencing control method is adopted. This method estimates the cooling load Q_{ch} by Eq. (13) and compares Q_{ch} with predefined thresholds *Qon/off z* to decide the on or off switch of chillers. Normally, a dead band should be adopted to avoid frequent switch triggering when the load fluctuates within a narrow interval [27]. The switch-on/off thresholds are calculated by Eqs. (14) and (15); a chiller and its corresponding pump(s) will be staged on when the instantaneous cooling load is greater than the threshold value for a certain time period; a chiller

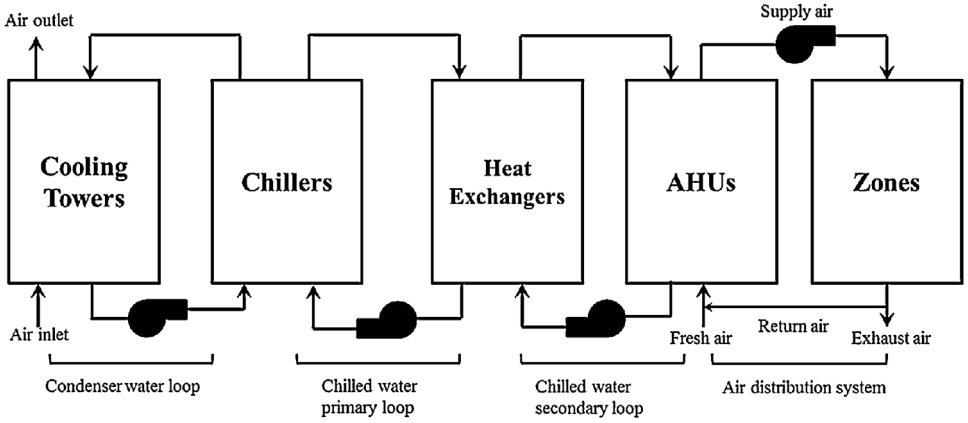

Fig. 2. Schematic of the complex AC system [26].

and its corresponding pump(s) will be staged off when the instantaneous cooling load is lower than the threshold value for a certain time period [28].

$$Q_{ch} = c_p m_w \left(T_{chw,rtn} - T_{chw,\sup}\right) \quad (13)$$

$$Q_z^{on} = z \times Q_{rated} \times (1 + dead\_band) \quad (14)$$

$$Q_z^{off} = (z-1) \times Q_{rated} \times (1 - dead\_band) \quad (15)$$

where c_p is the water specify heat; m_w is the mass flow rate of water; $T_{chw,rtn}$ and $T_{chw,sup}$ are the CHWR temperature and CHWS temperature; Q_z^{on} is the switch-on threshold; Q_z^{off} is the switch-off threshold; z is the number of chillers in operation; Q_{rated} is the nominal cooling capacity of one chiller (here, each chiller has the same rated cooling capacity); and *dead_band* is the dead band which is a user-defined value between 0 and 1.

3.1.2. Sequencing control of cooling towers

This is to determine the on or off switch of towers according to the heat amount that needs to be rejected. In practice, the operating cooling towers number N_{ct} is always coupled with the operating chillers as shown in Eq. (16), where k is a coefficient that normally depends on the chiller plant configuration.

$$N_{ct} = kN_{ch} \quad (16)$$

3.1.3. Controls of critical temperatures

Four critical temperatures are always under feedback control, including CWS temperature, CHWS from chillers, CHWS from heat exchangers and SA temperature. The SA temperature is maintained through modulating the water flow rate inside AHUs. The CWS temperature is controlled by changing the cooling tower fan frequency; the CHWS temperature from chiller(s) is maintained by changing the refrigerant flow rate; the CHWS temperature from heat exchanger(s) is controlled through modulating the water pump speed.

3.2. Simulation platform

The simulation platform was constructed by using the co-simulation between TRNSYS [29] and MATLAB (see Fig. 3.). The virtual AC system was established in TRNSYS, which was used to produce the online operation data. The optimization algorithm, introduced in Section 2.4, was realized in a separate MATLAB module. During every optimization process, the optimizer optimized the decision variables through minimizing the system total power requirement. Identified optimal values of the decision variables were sent to the virtual AC system to supervise its operation.

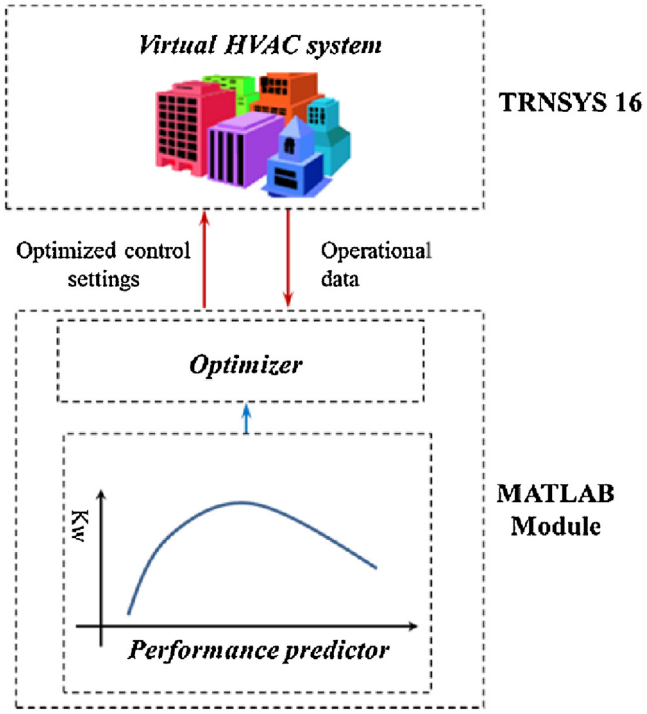

Fig. 3. Structure of co-simulation between TRNSYS and MATLAB.

The TRNSYS model was built based on a supertall building in Hong Kong. Six water-cooled centrifugal chillers were employed in the chiller plant, each of which has the capacity of 7230 kW. The rated water flow rates of the pumps for chilled water and cooling water circulation are 345 l/s and 410 l/s. Eleven cooling towers were used and the rated water flow is 250 l/s. The validated models of cooling towers, chillers and pumps established in [30] were used in this case study.

In local control loops, several PI/PID controllers were used to track the set-points. The PI controller with the parameters P = −0.95 and I = 35 s was used to control the fan speed of cooling towers so as to track the CWS temperature set-points. For the CHWS temperature from heat exchangers, the PID controller with the parameters P = −0.9, I = 10 s and D = 5 s was adopted to control the pump speed. An additional PI controller with the parameters P = −0.3 and I = 2 s was employed to track SA temperature. Controller parameters were kept constant under different optimization mechanisms and the trial-and-error method was used in controller tuning. The screen-shot of the established TRNSYS model is shown in Fig. 4. A 24-h

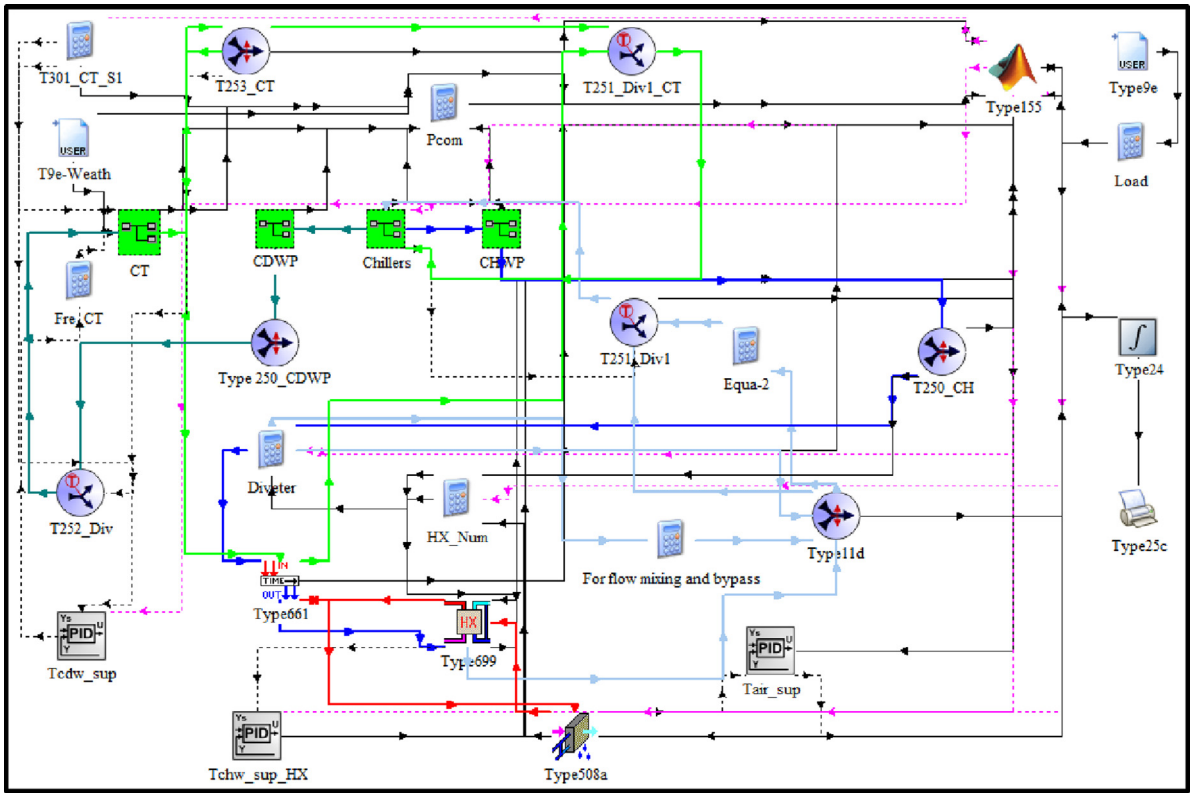

Fig. 4. TRNSYS model (screenshot).

Table 1
Major TRNSYS settings in "control cards".

Item	Value	Unit
Simulation start time	0	min
Simulation stop time	1440	min
Simulation time step	30	s
Solution method	Successive	/
The minimum relaxation factor	1	/
The maximum relaxation factor	1	/
Equation solver	0	/
Equation trace	False	/
Debug mode	False	/
Tolerance integration	0.001	dimensionless
Tolerance convergence	0.001	dimensionless
Tolerance value	Absolute	/

simulation time period was used with a time step of 30 s. Other settings are shown in Table 1.

3.3. Load profiles and operational constraints

The cooling load profiles of three days in 2013 were used, including a typical spring day (April 2013), a summer day (August 2013) and an autumn day (October 2013). These profiles were measured in a supertall building in Hong Kong. The peak value of the cooling load in the spring day was 6160 kW, occurred at 14:26; the peak value in the summer day was 23,706 kW, occurred at 9:14 (during precooling period); and the peak value in the autumn day was 15,360 kW, occurred at 16:01. The mean of the cooling load was 4598 kW for the spring day, 14,959 kW for the summer day and 10,038 kW for the autumn case. Figs. 5–7 give the cooling load profiles of the three days respectively. The corresponding daily weather profiles of the three days from Hong Kong Observatory were also plotted in Figs. 5–7 respectively. Basically, regarding the peak load and the mean air temperature, the spring case had the lowest cooling load; the autumn case was at the middle; while the summer case had the highest values.

Table 2
Threshold and boundary values used in the constraints Eqs. (7)–(12).

Parameter name	Value (°C)		
	spring	summer	autumn
$[T_{cw,low}, T_{cw,up}]$	[20,28]	[28,35]	[24,30]
$[T_{chw,prm,low}, T_{chw,prm,up}]$	[5,8]		
$[T_{chw,sec,low}, T_{chw,sec,up}]$	[6.5, 11.5]		
$[T_{sa,low}, T_{sa,up}]$	[12,18]		
ΔT_{Thres}	0.5		
ΔT_{min}	0.8		

The threshold and boundaries used in the constraints (Eqs. (7)–(12)) are listed in Table 2, where all the three cases have the same setting except the set-point range for the cooling water. The optimization problem (Eqs. (5) and (6)) with the constraints (Eqs. (7)–(12)) was solved by using an exhaustive search method. A temperature step change of 0.1 °C was adopted according to a previous study [31].

3.4. Two critical events

According to the chapter 42, "supervisory control strategies and optimization", of ASHRAE handbook [10] and the reference [32], the variation of the load condition has a significant effect on the optimal operation of chiller plants. Therefore, events should be defined to capture critical changes in the load condition. Following this logic, two events were defined. Event (1) (denoted as "PLR Change"): when the PLR changes by a significant amount since the last optimization, an action will be taken to optimize the control settings since previous settings may not be optimal; Event (2) (denoted as "Chiller On/Off"): when a chiller is switched on or off, the load dis-

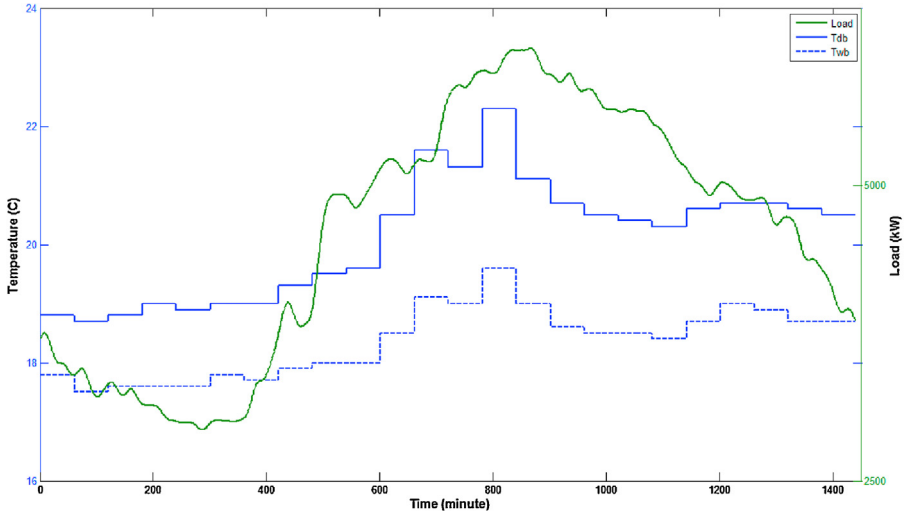

Fig. 5. The load profile of a spring day (the mean of the dry bulb temperature is 20.1 °C and the mean of the wet bulb temperature is18.4 °C).

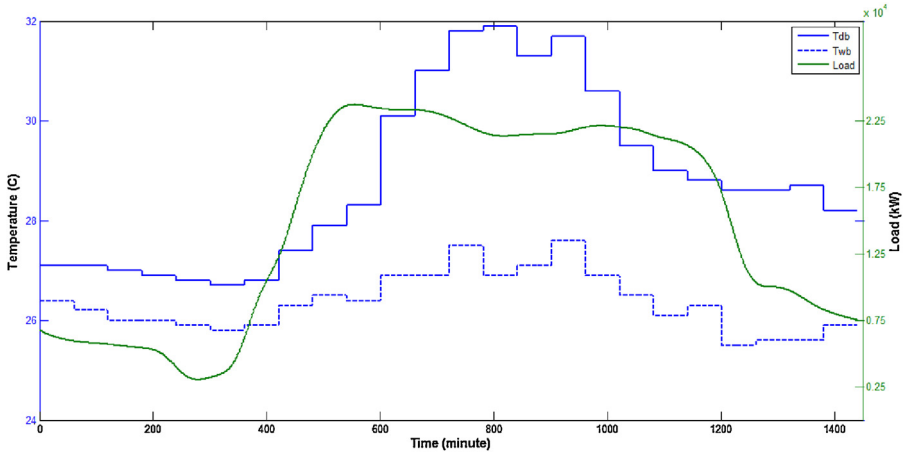

Fig. 6. The load profile of a summer day (the mean of the dry bulb temperature is 28.83 °C and the mean of the wet bulb temperature is 26.36 °C).

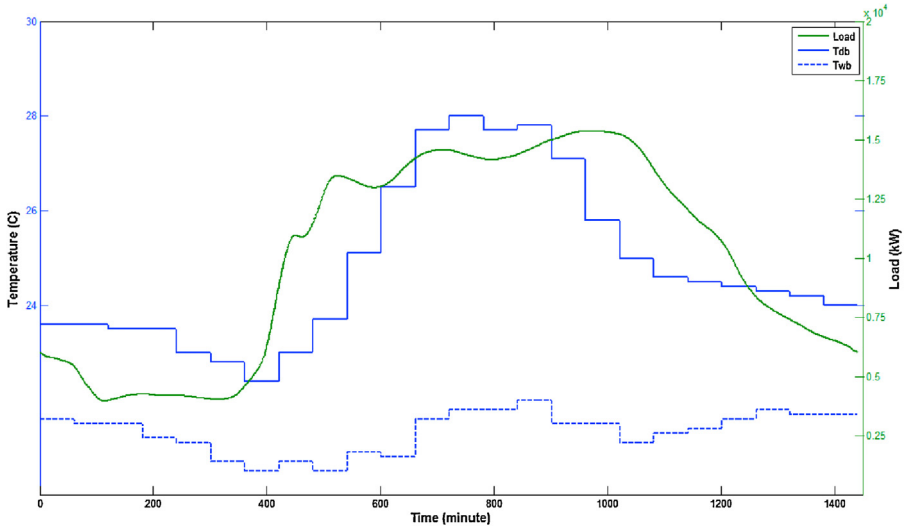

Fig. 7. The load profile of an autumn day (the mean of the dry bulb temperature is 24.83 °C and the mean of the wet bulb temperature 21.33 °CC).

tribution among chillers will have a sudden change, and thus an optimization is needed.

To validate the importance of the two events, computer simulation was carried out to access the importance of the events on the energy performance. The energy saving percentages (shown in Tables 4 and 6) were calculated based on the corresponding benchmark case, in which no optimization was conducted (details of benchmark settings are given in Section 4.3). In order to bench-

Table 3
Energy savings of event-based optimization using a single event "Chiller On/Off".

Op. methods	Energy saving	Ratio to time-driven optimization
spring case		
15 min	5.25%	/
Chiller On/Off	0.00%	
summer case		
15 min	11.27%	$\frac{8.82\%}{11.27\%} = 78.23\%$
Chiller On/Off	8.82%	
autumn case		
15 min	8.10%	$\frac{7.09\%}{8.10\%} = 87.50\%$
Chiller On/Off	7.09%	

Table 4
Energy savings of event-driven optimization using a single event "PLR Change by 7%".

Op. methods	Energy saving	Ratio to time-driven optimization
spring case		
15 min	5.25%	$\frac{4.76\%}{5.25\%} = 90.67\%$
PLR Change (threshold = 7%)	4.76%	
summer case		
15 min	11.27%	$\frac{10.55\%}{11.27\%} = 93.61\%$
PLR Change (threshold = 7%)	10.55%	
autumn case		
15 min	8.10%	$\frac{9.29\%}{8.10\%} = 114.69\%$
PLR Change (threshold = 7%)	9.29%	

mark the energy performance of single event, the energy saving percentages were compared with the conventional time-driven method (shown in Tables 4 and 6). Please note that the optimization frequency "every 15 min" (denoted as "15mins") was used for evaluation since it is a high optimization frequency in practice and enough for comparison.

Table 3 shows the importance of event 'Chiller On/Off' on energy consumption. The summer and autumn cases achieve 8.82% and 7.09% of the energy saving respectively, which are 78.23% and 87.5% of the corresponding energy saving achieved by the time-driven optimization. In the spring case, the operating chiller number did not change in 24-h operation because the load is relatively low, which results in a zero energy saving (no 'Chiller On/Off' event was triggered). Thus, in terms of energy saving, "Chiller On/Off" should be considered as a critical event. Please note that the "Chiller On/Off" is in the form of digital state and easy to identify.

The "PLR Change" is in the form of continuous state and needs a threshold in the event definition to reflect the state transition. Different values of the"PLR Change" threshold were tested, based on which a suitable threshold value was selected. Here the threshold values ranging from 5% to 15% were studied. Such range was set according to ASHRAE Handbook, which recommends 10% for the threshold of chilled-water load change (in Section 3.2 of Chapter 42). The results of the energy saving (in percentage) were also plotted in Figs. 8–10. It can be seen that energy saving percentage was not linear with the PLR threshold. The reason may be due to the nonlinear relationship between PLR and COP. It can be seen that the choice of the threshold is quite important in terms of the energy performance. As the event "PLR change by 7%" guaranteed a relatively good result in all the three cases, it was used as an event in the following study.

To benchmark the energy performance of this event, the energy saving percentage of the event-driven optimization using "PLR Change by 7%" was compared with the time-driven optimization. The results are listed in Table 4. The energy saving ratios of the event-driven optimization are 90.67%, 93.61% and 114.69% of the three cases respectively.

The above analysis demonstrated that both 'chiller on/off' and 'PLR change by 7%' had a significant influence on the performance of real-time optimization and therefore they were used as 'events' in the event-driven optimization in the following case studies.

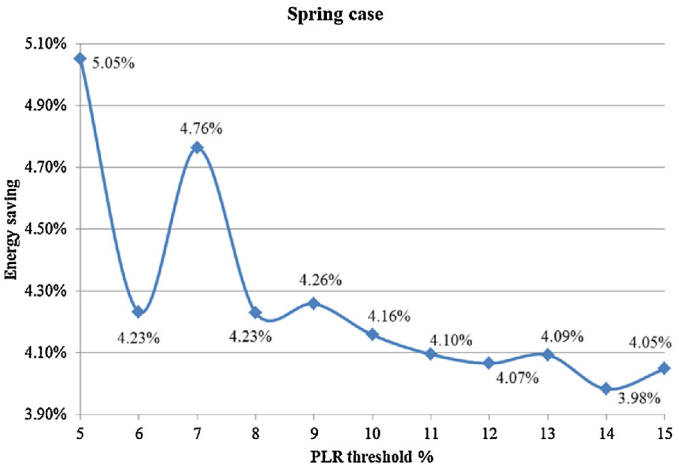

Fig. 8. Energy saving vs PLR threshold (spring case).

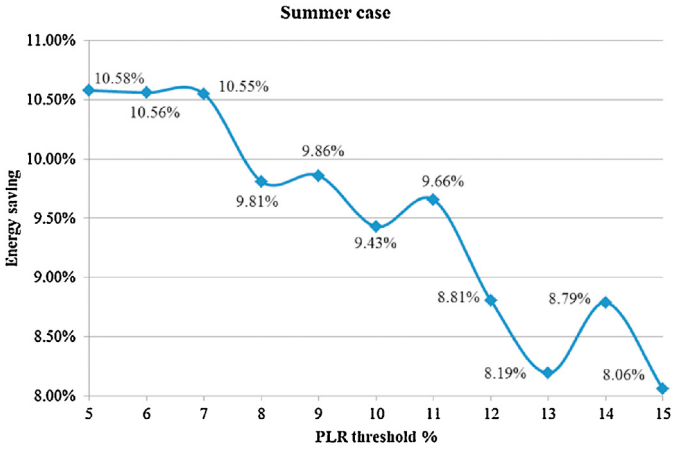

Fig. 9. Energy saving vs PLR threshold (summer case).

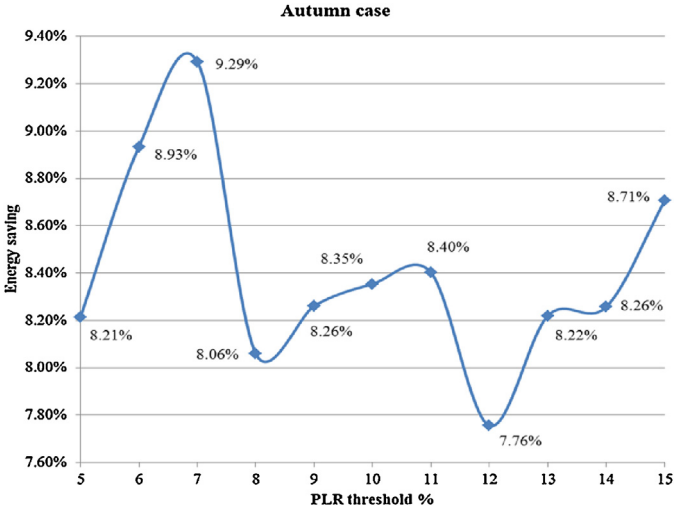

Fig. 10. Energy saving vs PLR threshold (autumn case).

Table 5
Energy performance of the time-driven and event-driven optimization methods.

Optimization methods	Power consumption (kWh)	Saving	Remark
spring case			
Benchmark	44486	0.00%	
2 h	42511	4.44%	
1 h	42398	4.89%	
30 min	42310	5.17%	
15 min	42185	5.25%	
Chiller On/Off & PLR Change	**42146**	**5.26%**	**PLR threshold = 7%**
summer case			
Benchmark	180356	0.00%	
2 h	165883	8.02%	
1 h	163784	9.19%	
30 min	161000	10.73%	
15 min	160026	11.27%	
Chiller On/Off & PLR Change	**159033**	**11.82%**	**PLR threshold = 7%**
autumn case			
Benchmark	110938	0.00%	
2 h	103852	6.39%	
1 h	102761	7.37%	
30 min	102418	7.68%	
15 min	101949	8.10%	
Chiller On/Off & PLR Change	**100399**	**9.50%**	**PLR threshold = 7%**

4. Results and analysis

The performance of the proposed event-driven optimization with the above two identified events was evaluated in simulations by two indices, namely, daily energy saving and computational load. The first one was used to indicate the energy performance, while the second one was to access the computational complexity of the optimization methods.

4.1. Energy performance comparison

The energy performance of the event-driven optimization was compared with the benchmark case, in which the decision variables, including the set-points of CWS temperature, CHWS temperature from chillers, CHWS temperature from heat exchangers and SA temperature, were fixed as constants. Benchmark settings were:

- the spring case, $T_{cw} = 26\,^{\circ}C, T_{chw,prm} = 7.5\,^{\circ}C, T_{chw,sec} = 9\,^{\circ}C, T_{sa} = 14\,^{\circ}C$;
- the summer case, $T_{cw} = 30\,^{\circ}C, T_{chw,prm} = 6\,^{\circ}C, T_{chw,sec} = 7.5\,^{\circ}C, T_{sa} = 15\,^{\circ}C$;
- the autumn case, $T_{cw} = 28\,^{\circ}C, T_{chw,prm} = 7\,^{\circ}C, T_{chw,sec} = 8.5\,^{\circ}C, T_{sa} = 14.5\,^{\circ}C$.

For the event-driven optimization, the threshold for the "PLR Change" was set to 7% in all these three cases. For the time-driven optimization, four different optimization frequencies were tested, 'every 2 h', 'every 1 h', 'every half hour' and "every 15 min". The energy consumption and energy saving percentage of all the cases were listed in Table 5.

It was observed that the energy consumption saving increases as the optimization frequency increases in the time-driven optimization, which agrees well with the perception that higher optimization frequency leads to higher energy consumption saving [17]. The event-driven method achieved the best energy saving among all the optimization methods. Compared with the benchmark, the energy savings were 5.26%, 11.82% and 9.50% in spring, summer and autumn cases. The main reason for these improvements is that the event-driven mechanism performed the optimizations at a more right time.

Table 6
Computation loads of the time-driven and event-driven methods.

Optimization methods	Op. times	Computation time (s)	Computation saving
spring case			
15 min (benchmark)	96	63.61	0.00%
Chiller On/Off & PLR Change	**13**	**10.51**	**83.48%***
summer case			
15 min (benchmark)	96	189.50	0.00%
Chiller On/Off & PLR Change	**45**	**76.51**	**59.63%**
autumn case			
15 min (benchmark)	96	122.00	0.00%
Chiller On/Off & PLR Change	**30**	**37.26**	**69.46%**

* The computation saving is calculated by $\left(1 - \frac{10.51}{63.61}\right) \times 100\%$.

4.2. Computation load comparison

The computation loads of the time-driven and event-driven optimization were compared in Table 6, which were measured by the time required by the optimization method in searching the optimal settings. As the case "every 15 min" had the highest computational load, it was used as the benchmark for computation load comparison. It can be seen that, compared with the benchmark, the event-driven optimization reduced the computation load significantly, saved by 83.48%, 59.63% and 69.46% in the spring, summer and autumn cases respectively. It should be noted that this achievement was obtained without sacrificing the energy performance. Actually, the energy performance of the event-driven optimization was superior to the benchmark (See Table 5).

4.3. Discussion and application issues

The above case studies showed that event-driven optimization may be a good alternative for the real-time optimization of HVAC systems (compared with the conventional time-driven optimization) as the operation conditions of HVAC systems experience stochastic changes. It should be noted that the validation was limited to a simulation study, focused only on the water side system of an HVAC system. To demonstrate the applicability of event-driven optimization in HVAC systems, case studies on other subsystems of HVAC systems and experiments are needed, which will be part of our future work.

The case studies also showed that a key factor to the success of the event-driven optimization is the definition of events. Defining proper "events" requires more sophisticated techniques compared to simply reacting to "time". Therefore, a systematic way of defining events will be another part of our future work, in which different ways, like prior knowledge, computer simulation or operational data analysis, will be investigated.

With the widely use of building automation system (BAS), the realization of event-driven optimization is not difficult when events are well defined and can be properly identified. This is because the optimization algorithm of the event-driven optimization is the same with that of the conventional time-driven optimization strategies.

5. Conclusions

An event-driven optimization for HVAC systems has been investigated in this study. Compared with a conventional time-driven optimization, the new method triggers the action of optimization using predefined events. As the event-driven optimization is able to capture the unpredictable changes in the system operating conditions, the optimization can be done in the 'right' time and therefore the energy performance can be guaranteed when compared with

the conventional time-driven optimization. In the case study, two events, "chiller on/off" and "PLR change", were defined from prior knowledge and used in a typical HVAC system; and the results showed that the event-driven optimization can reduce the computational load effectively (60–84%) without sacrificing the energy performance. Future work includes systematic studies of event definition of HVAC systems and tests of event-driven optimization numerically and experimentally on a comprehensive air- conditioning system.

Acknowledgement

The work described in this paper was fully supported by a grant from the Research Grants Council of the Hong Kong Special Administrative Region, China (Project No.124012).

References

[1] L. Pérez-Lombard, J. Ortiz, C. Pout, A review on buildings energy consumption information, Energy Build. 40 (2008) 394–398.
[2] L. Lu, W. Cai, L. Xie, S. Li, Y.C. Soh, HVAC system optimization—in-building section, Energy Build. 37 (2005) 11–22.
[3] J. Kao, Control strategies and building energy consumption, ASHRAE Trans. 91 (1985).
[4] Z. Cumali, Global optimization of HVAC system operations in real time, ASHRAE Trans. 94 (1988) 1729–1744.
[5] J. Braun, G. Diderrich, Near-optimal control of cooling towers for chilled-water systems, ASHRAE Trans. 96 (1990).
[6] Z. Cumali, Application of real-time optimization to building systems, ASHRAE Trans. 100 (1994).
[7] N. Nassif, S. Kajl, R. Sabourin, Optimization of HVAC control system strategy using two-objective genetic algorithm, HVAC&R Res. 11 (2005) 459–486.
[8] D. Fisk, Optimising heating system structure using exergy Branch and Bound, Build. Serv. Eng. Res. Technol. (2013) (pp. 0143624413489891).
[9] Y. Chang, W. Chen, C. Lee, C. Huang, Simulated annealing based optimal chiller loading for saving energy, Energy Convers. Manage. 47 (2006) 2044–2058.
[10] ASHRAE, Chapter 42 supervisory control strategies and optimization, in: ASHRAE Handbook – HVAC Applications, si edn, ASHRAE Inc., Atlanta, USA, 2015.
[11] S. Wang, Z. Ma, Supervisory and optimal control of building HVAC systems: a review, HVAC&R Res. 14 (2008) 3–32.
[12] A. Kusiak, M. Li, F. Tang, Modeling and optimization of HVAC energy consumption, Appl. Energy 87 (2010) 3092–3102.
[13] M. Mossolly, K. Ghali, N. Ghaddar, Optimal control strategy for a multi-zone air conditioning system using a genetic algorithm, Energy 34 (2009) 58–66.
[14] S. Yoon, C. Park, G. Augenbroe, On-line parameter estimation and optimal control strategy of a double-skin system, Build. Environ. 46 (2011) 1141–1150 (5).
[15] M. Zaheer-uddin, G.R. Zheng, Optimal control of time-scheduled heating, ventilating and air conditioning processes in buildings, Energy Convers. Manage. 41 (2000) 49–60 (1).
[16] J. Braun, S. Klein, W. Beckman, J. Mitchell, Methodologies for optimal control of chilled water systems without storage, ASHRAE Trans. 95 (1989) 652–662.
[17] S. Huang, W. Zuo, Optimization of the water-cooled chiller plant system operation, Optimization (2014).
[18] L. Lu, W. Cai, Y.S. Chai, L. Xie, Global optimization for overall HVAC systems—part I problem formulation and analysis, Energy Convers. Manage. 46 (2005) 999–1014.
[19] V.M. Zavala, Real-time optimization strategies for building systems, Ind. Eng. Chem. Res. 52 (2012) 3137–3150.
[20] J. Sandee, W. Heemels, P. Van Den Bosch, Case studies in event-driven control, in: Hybrid Systems: Computation and Control, Springer, 2007, 2007, pp. 762–765.
[21] Q. Liu, Z. Wang, X. He, D. Zhou, A survey of event-based strategies on control and estimation, Syst. Sci. Control Eng. 2 (2014) 90–97.
[22] C.G. Cassandras, Introduction to Discrete Event Systems, Springer Science & Business Media, 2008.
[23] C. Cassandras, Event-driven control, communication, and optimization, in: 32nd Chinese Control Conference (CCC), Xi'an, China, 2013, pp. 1–5.
[24] J.H. Sandee, Event-Driven Control in Theory and Practice: Trade-Offs in Software and Control Performance, Ph.D Dissertation, Eindhoven Univ. of Technology, Eindhoven, North Brabant, Netherlands, 2006.
[25] W. Heemels, J. Sandee, P. Van Den Bosch, Analysis of event-driven controllers for linear systems, Int. J. Control 81 (2008) 571–590.
[26] Y. Sun, G. Huang, Z. Li, S. Wang, Multiplexed optimization for complex air conditioning systems, Build. Environ. 65 (2013) 99–108.
[27] Y. Sun, S. Wang, F. Xiao, In situ performance comparison and evaluation of three chiller sequencing control strategies in a super high-rise building, Energy Build. 61 (2013) 333–343.
[28] Y. Liao, G. Huang, Y. Sun, L. Zhang, Uncertainty analysis for chiller sequencing control, Energy Build. 85 (2014) 187–198.
[29] TRNSYS, A transient systems simulation program, TRNSYS 16 (2006).
[30] S. Wang, Dynamic simulation of a building central chilling system and evaluation of EMCS on-line control strategies, Build. Environ. 33 (1998) 1–20.
[31] Z. Ma, S. Wang, An optimal control strategy for complex building central chilled water systems for practical and real-time applications, Build. Environ. 44 (2009) 1188–1198.
[32] S.B. Austin, Optimum chiller loading, Ashrae J. 33 (1991) 40–43.